

Uncertainty and Fuzzy Modeling in Human-robot Navigation

Rainer Palm and Achim J. Lilienthal

AASS, Dept. of Technology, Örebro University, SE-70182 Örebro, Sweden

Keywords: Human-robot Interaction, Navigation, Fuzzy Modeling, Gaussian Noise.

Abstract: The interaction between humans and mobile robots in shared areas requires a high level of safety especially at the crossings of the trajectories of humans and robots. We discuss the intersection calculation and its fuzzy version in the context of human-robot navigation with respect to noise information. Based on known parameters of the Gaussian input distributions at the orientations of human and robot the parameters of the output distributions at the intersection are to be found by analytical and fuzzy calculation. Furthermore the inverse task is discussed where the parameters of the output distributions are given and the parameters of the input distributions are searched. For larger standard deviations of the orientation signals we suggest mixed Gaussian models as approximation of nonlinear distributions.

1 INTRODUCTION

Activities of human operators and mobile robots in shared areas require a high degree of system stability and security. Planning of mobile robot tasks, navigation and obstacle avoidance were major research activities for many years (Khatib, 1985; Firl, 2014; Palm and Lilienthal, 2018). Using the same workspace at the same time requires adapting the behavior of human agents and robots to facilitate successful collaboration or support separate work for both. (O.H.Hamid and N.L.Smith, 2017) present a general discussion on robot-human interactions with the emphasis on cooperation. In this context, recognizing human intentions to achieve a particular goal is an important issue reported by (Tahboub, 2006; Fraichard et al., 2014; Palm et al., 2016; Palm and Iliev, 2007). The problem of crossing trajectories between humans and robots is addressed by Bruce et al. who describe a planned human - robot rendezvous at an intersection zone (Bruce et al., 2015). In this connection the goal to achieve more natural human-robot interactions is obtained by human-like sensor systems as they share their functional principle with natural systems (Robertsson et al., 2007; Palm and Iliev, 2006; Kassner et al., 2014). Based on an estimate of the positions and orientations of robot and human, the intersections of the intended linear trajectories of robot and human are calculated. Due to system uncertainties and observation noise, the intersection estimates are also corrupted by noise. In (W.Luo et al., 2014) and (J.Chen et al., 2018) a multiple tar-

get tracking approach for robots and other agents are discussed from the point of view of a higher control level. In our paper we concentrate on the one-robot one-human case in order to go deeper into the problem of accuracy and collision avoidance in the case of short distances between the acting agents. Depending on the distance between human and robot, uncertainties in the orientation between human and robot with standard deviations of more than one degree can lead to high uncertainties at the points of intersection. For security reasons and for effective cooperation between human and robot, it is therefore essential to predict uncertainties at possible crossing points. The relationship between the position and orientation of the human/robot and the intersection coordinates is non-linear, but can be linearized under certain constraints. This is especially true if we only consider the linear part of correlation between input and output of a nonlinear transfer element (R.Palm and Driankov, 1993; Banelli, 2013) and for small standard deviations at the input. For fuzzy systems two main directions to deal with uncertain system inputs are the following: One direction is the processing of fuzzy inputs (inputs that are fuzzy sets) in fuzzy systems (R.Palm and Driankov, 1994; L.Foulloy and S.Galichet, 2003; H.Hellendoorn and R.Palm, 1994). Another direction is the fuzzy reasoning with probabilistic inputs (Yager and Filev, 1994) and the transformation of probabilistic distributions into fuzzy sets (Pota et al., 2011). Both approaches fail more or less to solve the practical problem of processing a probabilistic distribution through a static nonlinear system

that is both analytically and fuzzily described. The motivation to deal with uncertain/fuzzy inputs in an analytical way is to predict future situations such as collisions at specific areas and to use this information for feed forward control actions and re-planning of trajectories. In the case of a static fuzzy system we have to deal with fuzzy problems twofold: the fuzzy system itself in form of a set of fuzzy rules and an input signal being interpreted as fuzzy input. This is especially important when human agents come into play whose intentions, actions and reactions are difficult to predict and interpret by a robot. There are many issues to consider in this context but the point to avoid collisions or enable cooperations between human and robot is one of the basic issues that is going to be discussed. Therefore in this paper we address the following *direct task*: given the parameters of Gaussian distributions at the input of a fuzzy system, find the corresponding parameters of the output distributions. The *inverse task* means: Given the output distribution parameters, find the input distribution parameters. An application is the bearing task for intersections of possible trajectories emanating from different positions for the same target. In the following we restrict our consideration to the static case in order to show the general problems and difficulties. In the context of larger standard deviations at the input, we address the case of mixed Gaussian distributions. The paper is organized as follows. Section 2 deals with Gaussian noise and the bearing problem in general and its analytical approach. In Section 3 the inverse problem is addressed that is to find the input distribution parameters while the output parameters are given. Section 4 deals with the local linear fuzzy approximation of the nonlinear analytical calculation. In Section 5 the extension from two orientation inputs to another four position inputs is discussed. In Section 6 mixed Gaussian distributions and their contribution to the intersection problem are presented. Section 7 deals with simulations to show the influence of the resolution of the fuzzy system on the accuracy at the system output. Finally, Section 8 concludes the paper.

2 GAUSSIAN NOISE AND THE BEARING PROBLEM

2.1 Computation of Intersections - Analytical Approach

The following computation deals with the intersection (x_c, y_c) of two linear paths $\mathbf{x}_R(t)$ and $\mathbf{x}_H(t)$ in a plane along which robot and human intend to move. $\mathbf{x}_H =$

(x_H, y_H) and $\mathbf{x}_R = (x_R, y_R)$ are the position of human and robot and ϕ_H and ϕ_R their orientation angles (see Figs. 1 and 2).

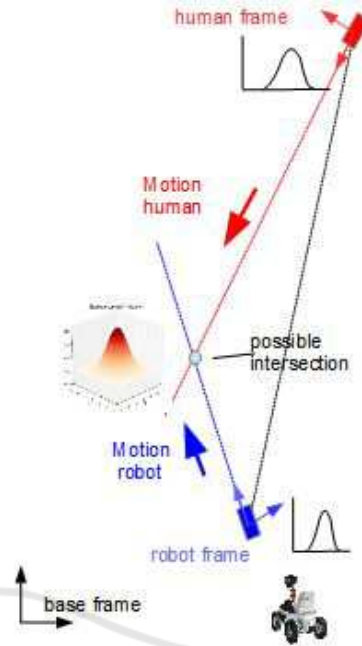


Figure 1: Human-robot scenario.

Then we have the relations

$$\begin{aligned} x_H &= x_R + d_{RH} \cos(\phi_R + \delta_R) \\ y_H &= y_R + d_{RH} \sin(\phi_R + \delta_R) \\ x_R &= x_H + d_{RH} \cos(\phi_H + \delta_H) \\ y_R &= y_H + d_{RH} \sin(\phi_H + \delta_H) \end{aligned} \quad (1)$$

where positive angles δ_H and δ_R are measured from the y coordinates counterclockwise. Angle $\tilde{\beta} = \pi - \delta_R - \delta_H$ is the angle at the intersection.

The variables \mathbf{x}_H , \mathbf{x}_R , ϕ_R , δ_H , δ_R , d_{RH} and the angle γ are supposed to be measurable. The unknown orientation angle ϕ_H is computed by

$$\phi_H = \arcsin((y_H - y_R)/d_{RH}) - \delta_H + \pi \quad (2)$$

After some substitutions we obtain the coordinates x_c and y_c straight forward

$$\begin{aligned} x_c &= \frac{A - B}{\tan \phi_R - \tan \phi_H} \\ y_c &= \frac{A \tan \phi_H - B \tan \phi_R}{\tan \phi_R - \tan \phi_H} \\ A &= x_R \tan \phi_R - y_R \\ B &= x_H \tan \phi_H - y_H \end{aligned} \quad (3)$$

Rewriting (3) leads to

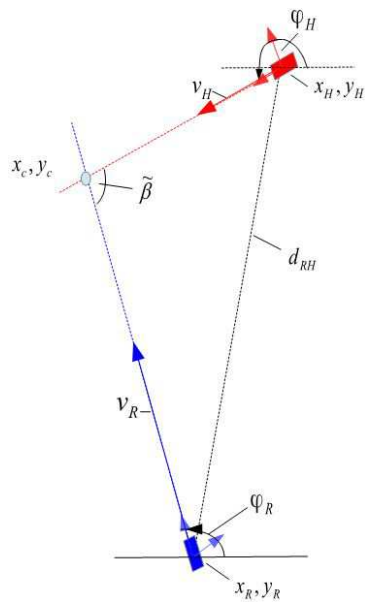


Figure 2: Human-robot scenario: geometry.

$$\begin{aligned}
 x_c &= \left(x_R \frac{\tan \phi_R}{G} - y_R \frac{1}{G} \right) - \left(x_H \frac{\tan \phi_H}{G} - y_H \frac{1}{G} \right) \\
 y_c &= \left(x_R \frac{\tan \phi_R \tan \phi_H}{G} - y_R \frac{\tan \phi_H}{G} \right) \\
 &\quad - \left(x_H \frac{\tan \phi_H \tan \phi_R}{G} - y_H \frac{\tan \phi_R}{G} \right) \\
 G &= \tan \phi_R - \tan \phi_H
 \end{aligned} \tag{4}$$

which is a form that can be used for the fuzzification of (3)

Having a look at (4) we see that $\mathbf{x}_c = (x_c, y_c)^T$ is linear in $\mathbf{x}_{RH} = (x_R, y_R, x_H, y_H)^T$

$$\mathbf{x}_c = A_{RH} \cdot \mathbf{x}_{RH} \tag{5}$$

where

$$A_{RH} = f(\phi_R, \phi_H) = \frac{1}{G} \begin{pmatrix} \tan \phi_R & -1 & -\tan \phi_H & 1 \\ \tan \phi_R \tan \phi_H & -\tan \phi_H & -\tan \phi_R \tan \phi_H & \tan \phi_H \end{pmatrix}$$

To achieve the orientation of the human operator a scenario is recorded by human eye tracking plus a corresponding camera picture that is taken from the human's position and sent to the robot (Palm and Lilienthal, 2018). The robot measures its own position/orientation and the human's position. From the human's screen-shot the robot calculates

- orientation of human
- expected intersection
- direction of human's gaze to robot or object
- position of object

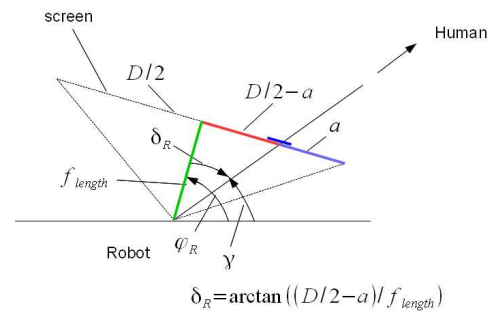


Figure 3: Camera geometry.

From the robot's point of view a picture from the scene is taken from which we obtain a projection of the human image onto the camera screen(see Fig. 3). From the focal length f_{length} , the width D of the screen and the distance a , an angle δ_R is computed

$$\delta_R = \arctan((D/2 - a)/f_{length}) \tag{6}$$

from which the orientation angle ϕ_H of the human is calculated (see also Fig. 2) and (2)

The TS-fuzzy approximation of (5) is given by (Palm and Lilienthal, 2018)

$$\mathbf{x}_c = \sum_{i,j} w_i(\phi_R) w_j(\phi_H) \cdot A_{RH,i,j} \cdot \mathbf{x}_{RH} \tag{7}$$

$w_i(\phi_R), w_j(\phi_H) \in [0, 1]$ are normalized membership functions with $\sum_i w_i(\phi_R) = 1$ and $\sum_j w_j(\phi_H) = 1$. The following paragraph deals with the accuracy of the computed intersection in the case of distorted orientation information.

2.2 Transformation of Gaussian Distributions

2.2.1 General Considerations

Let us consider a static nonlinear system

$$\mathbf{z} = F(\mathbf{x}) \tag{8}$$

with two inputs $\mathbf{x} = (x_1, x_2)^T$ and two outputs $\mathbf{z} = (z_1, z_2)^T$ where F denotes a nonlinear system. Let further the uncorrelated Gaussian distributed inputs x_1 and x_2 be described by the 2-dim density

$$f_{x_1, x_2} = \frac{1}{2\pi\sigma_{x_1}\sigma_{x_2}} \exp\left(-\frac{1}{2}\left(\frac{e_{x_1}^2}{\sigma_{x_1}^2} + \frac{e_{x_2}^2}{\sigma_{x_2}^2}\right)\right) \tag{9}$$

where $e_{x_1} = x_1 - \bar{x}_1$, \bar{x}_1 - mean(x_1), σ_{x_1} - standard deviation x_1 and $e_{x_2} = x_2 - \bar{x}_2$, \bar{x}_2 - mean(x_2), σ_{x_2} - standard deviation x_2 .

The question arises how the output signals z_1 and z_2 are distributed in order to obtain their standard deviations and the correlation coefficient between the

outputs. For linear systems Gaussian distributions are linearly transformed which means that the output signals are also Gaussian distributed. In general, this does not apply for nonlinear system as in our case. However, if we assume the input standard deviations small enough then we can construct local linear transfer functions for which the output distributions are Gaussian distributed but with correlated output components.

$$f_{z_1, z_2} = \frac{1}{2\pi\sigma_{z_1}\sigma_{z_2}\sqrt{1-\rho_{z_{12}}^2}} \cdot \exp\left(-\frac{1}{2(1-\rho_{z_{12}}^2)}\left(\frac{e_{z_1}^2}{\sigma_{z_1}^2} + \frac{e_{z_2}^2}{\sigma_{z_2}^2} - \frac{2\rho_{z_{12}}e_{z_1}e_{z_2}}{\sigma_{z_1}\sigma_{z_2}}\right)\right) \quad (10)$$

$\rho_{z_{12}}$ - correlation coefficient.

2.2.2 Differential Approach

Function F can be described by individual smooth and nonlinear static transfer functions (see block scheme 4) where $(x_1, x_2) = (\phi_R, \phi_H)$ and $(z_1, z_2) = (x_c, y_c)$

$$\begin{aligned} z_1 &= f_1(x_1, x_2) \\ z_2 &= f_2(x_1, x_2) \end{aligned} \quad (11)$$

Linearization of (11) yields

$$dz = \tilde{J} \cdot dx \quad \text{or} \quad \mathbf{e}_z = \tilde{J} \cdot \mathbf{e}_x \quad (12)$$

with

$$\begin{aligned} \mathbf{e}_z &= (e_{z_1}, e_{z_2})^T \quad \text{and} \quad \mathbf{e}_x = (e_{x_1}, e_{x_2})^T \\ dz &= (dz_1, dz_2)^T \quad \text{and} \quad dx = (dx_1, dx_2)^T \end{aligned} \quad (13)$$

$$\tilde{J} = \begin{pmatrix} \frac{\partial f_1}{\partial x_1} & \frac{\partial f_1}{\partial x_2} \\ \frac{\partial f_2}{\partial x_1} & \frac{\partial f_2}{\partial x_2} \end{pmatrix} \quad (14)$$

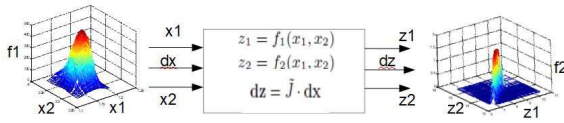


Figure 4: Differential transformation.

2.2.3 Specific Approach to the Intersection

In addition to the exact solution (4) we look at the differential approach. This is important if the contributing agents change their directions of motion. A further aspect is to quantify the uncertainty of \mathbf{x}_c in the presence uncertain angles ϕ_R and ϕ_H or in $\mathbf{x}_{RH} = (x_R, y_R, x_H, y_H)^T$.

Differentiating (4) with $\mathbf{x}_{RH} = \text{const.}$ yields

$$\begin{aligned} \dot{\mathbf{x}}_c &= \tilde{J} \cdot \dot{\phi} \\ \dot{\phi} &= (\dot{\phi}_R \quad \dot{\phi}_H)^T; \quad \tilde{J} = \begin{pmatrix} \tilde{J}_{11} & \tilde{J}_{12} \\ \tilde{J}_{21} & \tilde{J}_{22} \end{pmatrix} \end{aligned} \quad (15)$$

where

$$\begin{aligned} \tilde{J}_{11} &= \begin{pmatrix} -\tan\phi_H & 1 & \tan\phi_H & -1 \end{pmatrix} \frac{\mathbf{x}_{RH}}{G^2 \cdot \cos^2\phi_R} \\ \tilde{J}_{12} &= \begin{pmatrix} \tan\phi_R & -1 & -\tan\phi_R & 1 \end{pmatrix} \frac{\mathbf{x}_{RH}}{G^2 \cdot \cos^2\phi_H} \\ \tilde{J}_{21} &= \tilde{J}_{11} \cdot \tan\phi_H \\ \tilde{J}_{22} &= \tilde{J}_{12} \cdot \tan\phi_R \end{aligned}$$

2.2.4 Output Distribution

To obtain the density f_{z_1, z_2} of the output signal we invert (13) and substitute the entries of \mathbf{e}_x into (9)

$$\mathbf{e}_x = J \cdot \mathbf{e}_z \quad (16)$$

with $J = \tilde{J}^{-1}$ and

$$J = \begin{pmatrix} J_{11} & J_{12} \\ J_{21} & J_{22} \end{pmatrix} = \begin{pmatrix} \mathbf{j}_{xz} \\ \mathbf{j}_{yz} \end{pmatrix} \quad (17)$$

where $\mathbf{j}_{xz} = (J_{11}, J_{12})$ and $\mathbf{j}_{yz} = (J_{21}, J_{22})$. Entries J_{ij} are the result of the inversion of \tilde{J} . From this substitution which we get

$$\begin{aligned} f_{x_1, x_2} &= K_{x_1, x_2} \cdot \\ \exp\left(-\frac{1}{2} \cdot \mathbf{e}_z^T \cdot (\mathbf{j}_{x_1, z}^T, \mathbf{j}_{x_2, z}^T) \cdot S_x^{-1} \cdot \begin{pmatrix} \mathbf{j}_{x_1, z} \\ \mathbf{j}_{x_2, z} \end{pmatrix} \cdot \mathbf{e}_z\right) \end{aligned} \quad (18)$$

where $K_{x_1, x_2} = \frac{1}{2\pi\sigma_{x_1}\sigma_{x_2}}$ and

$$S_x^{-1} = \begin{pmatrix} \frac{1}{\sigma_{x_1}^2} & 0 \\ 0 & \frac{1}{\sigma_{x_2}^2} \end{pmatrix} \quad (19)$$

The exponent of (18) is rewritten into

$$\begin{aligned} xpo &= -\frac{1}{2} \cdot \left(\frac{1}{\sigma_{x_1}^2} (e_{z_1} J_{11} + e_{z_2} J_{12})^2 \right. \\ &\quad \left. + \frac{1}{\sigma_{x_2}^2} (e_{z_1} J_{21} + e_{z_2} J_{22})^2\right) \end{aligned} \quad (20)$$

and furthermore

$$\begin{aligned} xpo &= -\frac{1}{2} \cdot \left[e_{z_1}^2 \left(\frac{J_{11}^2}{\sigma_{x_1}^2} + \frac{J_{21}^2}{\sigma_{x_2}^2}\right) + e_{z_2}^2 \left(\frac{J_{12}^2}{\sigma_{x_1}^2} + \frac{J_{22}^2}{\sigma_{x_2}^2}\right) \right. \\ &\quad \left. + 2 \cdot e_{z_1} e_{z_2} \left(\frac{J_{11} J_{12}}{\sigma_{x_1}^2} + \frac{J_{21} J_{22}}{\sigma_{x_2}^2}\right) \right] \end{aligned} \quad (21)$$

Now, we compare x_{po} in (21) with the exponent in (10) of the output density (10)

Let

$$A = \left(\frac{J_{11}^2}{\sigma_{x_1}^2} + \frac{J_{21}^2}{\sigma_{x_2}^2}\right); \quad B = \left(\frac{J_{12}^2}{\sigma_{x_1}^2} + \frac{J_{22}^2}{\sigma_{x_2}^2}\right)$$

$$C = \left(\frac{J_{11}J_{12}}{\sigma_{x_1}^2} + \frac{J_{21}J_{22}}{\sigma_{x_2}^2}\right) \quad (22)$$

then a comparison of x_{po} in (21) and the exponent in (10) yields

$$\frac{1}{(1-\rho_{z_{12}}^2)} \frac{1}{\sigma_{z_1}^2} = A; \quad \frac{1}{(1-\rho_{z_{12}}^2)} \frac{1}{\sigma_{z_2}^2} = B$$

$$\frac{-2\rho_{z_{12}}}{(1-\rho_{z_{12}}^2)} \frac{1}{\sigma_{z_1}\sigma_{z_2}} = 2C \quad (23)$$

from which we finally get the correlation coefficient $\rho_{z_{12}}$ and the standard deviations σ_{z_1} and σ_{z_2}

$$\rho_{z_{12}} = -\frac{C}{\sqrt{AB}}$$

$$\frac{1}{\sigma_{z_1}^2} = A - \frac{C^2}{B}; \quad \frac{1}{\sigma_{z_2}^2} = B - \frac{C^2}{A} \quad (24)$$

So once we have obtained the parameters of the input distribution and the mathematical expression for the transfer function $F(x, y)$ we can compute the output distribution parameters directly.

3 INVERSE SOLUTION

In the previous presentation we discussed the problem: Given the parameters of the input distributions of a nonlinear system, find the parameters of the output distributions. In a bearing task that runs from different positions for the same target it might be helpful to define a particular bearing accuracy while finding out the necessary accuracy of the bearing instruments with regard their bearing angles.

This inverse task we apply is similar to that we discussed in section 2.2.2. The starting point is equation (13). Equations (10) describe the densities of the inputs and the outputs, respectively. Then we substitute (13) into (10) and discuss the exponent x_{po_z} only

$$x_{po_z} = \frac{-1}{2(1-\rho_{z_{12}}^2)} (\mathbf{e}_x^T \tilde{J}^T S_z^{-1} \tilde{J} \mathbf{e}_x - \frac{2\rho_{z_{12}} e_{z_1} e_{z_2}}{\sigma_{z_1} \sigma_{z_2}}) \quad (25)$$

where

$$S_z^{-1} = \begin{pmatrix} \frac{1}{\sigma_{z_1}^2}, 0 \\ 0, \frac{1}{\sigma_{z_2}^2} \end{pmatrix} \quad (26)$$

With

$$e_{z_1} e_{z_2} = (\tilde{J}_{11} e_{x_1} + \tilde{J}_{12} e_{x_2}) \cdot (\tilde{J}_{21} e_{x_1} + \tilde{J}_{22} e_{x_2});$$

$$\mathbf{e}_x^T \tilde{J}^T S_z^{-1} \tilde{J} \mathbf{e}_x =$$

$$e_{x_1}^2 \left(\frac{\tilde{J}_{11}^2}{\sigma_{z_1}^2} + \frac{\tilde{J}_{21}^2}{\sigma_{z_2}^2}\right) + e_{x_2}^2 \left(\frac{\tilde{J}_{12}^2}{\sigma_{z_1}^2} + \frac{\tilde{J}_{22}^2}{\sigma_{z_2}^2}\right)$$

$$+ 2e_{x_1} e_{x_2} \left(\frac{\tilde{J}_{11}\tilde{J}_{12}}{\sigma_{z_1}^2} + \frac{\tilde{J}_{21}\tilde{J}_{22}}{\sigma_{z_2}^2}\right) \quad (27)$$

we obtain for the exponent x_{po_z}

$$x_{po_z} = -\frac{1}{2(1-\rho_{z_{12}}^2)} \left(e_{x_1}^2 \left(\frac{\tilde{J}_{11}^2}{\sigma_{z_1}^2} + \frac{\tilde{J}_{21}^2}{\sigma_{z_2}^2}\right) + e_{x_2}^2 \left(\frac{\tilde{J}_{12}^2}{\sigma_{z_1}^2} + \frac{\tilde{J}_{22}^2}{\sigma_{z_2}^2}\right) + 2e_{x_1} e_{x_2} \left(\frac{\tilde{J}_{11}\tilde{J}_{12}}{\sigma_{z_1}^2} + \frac{\tilde{J}_{21}\tilde{J}_{22}}{\sigma_{z_2}^2}\right) - \frac{2\rho_{z_{12}}}{\sigma_{z_1}\sigma_{z_2}} (\tilde{J}_{11} e_{x_1} + \tilde{J}_{12} e_{x_2}) \cdot (\tilde{J}_{21} e_{x_1} + \tilde{J}_{22} e_{x_2}) \right) \quad (28)$$

and further

$$x_{po_z} = -\frac{1}{2} \left(e_{x_1}^2 \left(\frac{\tilde{J}_{11}^2}{\sigma_{z_1}^2} + \frac{\tilde{J}_{21}^2}{\sigma_{z_2}^2} - \frac{2\rho_{z_{12}} \tilde{J}_{11}\tilde{J}_{21}}{\sigma_{z_1}\sigma_{z_2}} \right) / (1-\rho_{z_{12}}^2) + e_{x_2}^2 \left(\frac{\tilde{J}_{12}^2}{\sigma_{z_1}^2} + \frac{\tilde{J}_{22}^2}{\sigma_{z_2}^2} - \frac{2\rho_{z_{12}} \tilde{J}_{12}\tilde{J}_{22}}{\sigma_{z_1}\sigma_{z_2}} \right) / (1-\rho_{z_{12}}^2) + \frac{2e_{x_1} e_{x_2}}{(1-\rho_{z_{12}}^2)} \cdot \left(\frac{\tilde{J}_{11}\tilde{J}_{12}}{\sigma_{z_1}^2} + \frac{\tilde{J}_{21}\tilde{J}_{22}}{\sigma_{z_2}^2} - \frac{\rho_{z_{12}}}{\sigma_{z_1}\sigma_{z_2}} (\tilde{J}_{11}\tilde{J}_{22} + \tilde{J}_{12}\tilde{J}_{21}) \right) \right) \quad (29)$$

Now, comparing (29) with the exponent of (10) of the input density we find that the mixed term in (29) should be zero from which we obtain the correlation coefficient and the standard deviations of the inputs

$$\rho_{z_{12}} = \left(\frac{\tilde{J}_{11}\tilde{J}_{12}}{\sigma_{z_1}^2} + \frac{\tilde{J}_{21}\tilde{J}_{22}}{\sigma_{z_2}^2}\right) \frac{\sigma_{z_1}\sigma_{z_2}}{(\tilde{J}_{11}\tilde{J}_{22} + \tilde{J}_{12}\tilde{J}_{21})} \quad (30)$$

$$\frac{1}{\sigma_x^2} = \left(\frac{\tilde{J}_{11}^2}{\sigma_{z_1}^2} + \frac{\tilde{J}_{21}^2}{\sigma_{z_2}^2} - \frac{2\rho_{z_{12}} \tilde{J}_{11}\tilde{J}_{21}}{\sigma_{z_1}\sigma_{z_2}}\right) / (1-\rho_{z_{12}}^2) \quad (31)$$

$$\frac{1}{\sigma_y^2} = \left(\frac{\tilde{J}_{12}^2}{\sigma_{z_1}^2} + \frac{\tilde{J}_{22}^2}{\sigma_{z_2}^2} - \frac{2\rho_{z_{12}} \tilde{J}_{12}\tilde{J}_{22}}{\sigma_{z_1}\sigma_{z_2}}\right) / (1-\rho_{z_{12}}^2) \quad (32)$$

4 FUZZY SOLUTION

The previous presentation shows that the computation of the output distribution can be associated with high costs which might be problematic especially in the on-line case. Provided that an analytical representation (8) is available then we can build a TS fuzzy model by the following rules R_{ij}

$$\begin{aligned}
 & R_{ij} : \\
 \text{IF } & x_1 = X_{1i} \text{ AND } x_2 = X_{2i} \\
 \text{THEN } & \rho_{z_{12}} = -\frac{C_{ij}}{\sqrt{A_{ij}B_{ij}}} \\
 \text{AND} & \\
 & \frac{1}{\sigma_{z_1}^2} = A_{ij} - \frac{C_{ij}^2}{B_{ij}}; \\
 \text{AND} & \\
 & \frac{1}{\sigma_{z_2}^2} = B_{ij} - \frac{C_{ij}^2}{A_{ij}}
 \end{aligned} \tag{33}$$

where X_{1i}, X_{2i} are fuzzy terms for x_1, x_2 , A_{ij}, B_{ij}, C_{ij} are functions of predefined variables $x_1 = x_{1i}$ and $x_2 = x_{2i}$

From (33) we get

$$\begin{aligned}
 \rho_{z_{12}} &= -\sum_{ij} w_i(x_1)w_j(x_2) \frac{C_{ij}}{\sqrt{A_{ij}B_{ij}}} \\
 \frac{1}{\sigma_{z_1}^2} &= \sum_{ij} w_i(x_1)w_j(x_2) \left(A_{ij} - \frac{C_{ij}^2}{B_{ij}} \right) \\
 \frac{1}{\sigma_{z_2}^2} &= \sum_{ij} w_i(x_1)w_j(x_2) \left(B_{ij} - \frac{C_{ij}^2}{A_{ij}} \right)
 \end{aligned} \tag{34}$$

$w_i(x_1) \in [0, 1]$ and $w_j(x_2) \in [0, 1]$ are weighting functions with $\sum_i w_i(x_1) = 1$ $\sum_j w_j(x_2) = 1$

5 EXTENSION TO SIX INPUTS AND TWO OUTPUTS

The previous section dealt with two orientation inputs and two intersection position outputs where the position coordinates of robot and human are assumed to be constant. Let us again consider the nonlinear system

$$\mathbf{x}_c = F(\mathbf{x}) \tag{35}$$

where F denotes a nonlinear system. Here we have 6 inputs $\mathbf{x} = (x_1, x_2, x_3, x_4, x_5, x_6)^T$ and 2 outputs $\mathbf{x}_c = (x_c, y_c)^T$. For the bearing problem we get $\mathbf{x} = (\phi_R, \phi_H, x_R, y_R, x_H, y_H)$

Let further the uncorrelated Gaussian distributed inputs $x_1 \dots x_6$ be described by the 6-dim density

$$f_{x_i} = \frac{1}{(2\pi)^{6/2} |S_x|^{1/2}} \exp\left(-\frac{1}{2} (\mathbf{e}_x^T S_x^{-1} \mathbf{e}_x)\right) \tag{36}$$

where $\mathbf{e}_x = (e_{x1}, e_{x2}, \dots, e_{x6})^T$; $\mathbf{e}_x = \mathbf{x} - \bar{\mathbf{x}}$, $\bar{\mathbf{x}}$ - mean(\mathbf{x}), S_x - covariance matrix.

$$S_x = \begin{pmatrix} \sigma_{x_1}^2 & 0 & \dots & 0 \\ 0 & \sigma_{x_2}^2 & \dots & 0 \\ \dots & \dots & \dots & \dots \\ 0 & \dots & 0 & \sigma_{x_6}^2 \end{pmatrix}$$

The output density is again described by

$$f_{x_c, y_c} = \frac{1}{2\pi \sigma_{x_c} \sigma_{y_c} \sqrt{1 - \rho^2}} \cdot \exp\left(-\frac{1}{2(1 - \rho^2)} (\mathbf{e}_{x_c}^T S_c^{-1} \mathbf{e}_{x_c} - \frac{2\rho e_{x_c} e_{y_c}}{\sigma_{x_c} \sigma_{y_c}})\right) \tag{37}$$

ρ - correlation coefficient.

In correspondence to (8) and (11) function F can be described by

$$x_c = f_1(\mathbf{x}) \tag{38}$$

$$y_c = f_2(\mathbf{x})$$

Furthermore we have in correspondence to (15)

$$\mathbf{e}_{x_c} = \tilde{J} \cdot \mathbf{e}_x \tag{39}$$

with

$$\tilde{J} = \begin{pmatrix} \tilde{J}_{11} & \tilde{J}_{12} & \dots & \tilde{J}_{16} \\ \tilde{J}_{21} & \tilde{J}_{22} & \dots & \tilde{J}_{26} \end{pmatrix} \tag{40}$$

where

$$\tilde{J}_{ij} = \frac{\partial f_i}{\partial x_j}, \quad i = 1, 2, \quad j = 1, \dots, 6 \tag{41}$$

Inversion of (40) leads to

$$\mathbf{e}_x = \tilde{J}^t \cdot \mathbf{e}_{x_c} = J \cdot \mathbf{e}_{x_c} \tag{42}$$

with the pseudo inverse $\tilde{J}^t = J$ of \tilde{J}

$$J = \begin{pmatrix} J_{11} & J_{12} \\ \dots & \dots \\ J_{61} & J_{62} \end{pmatrix} \tag{43}$$

where

$$S_c^{-1} = \begin{pmatrix} \frac{1}{\sigma_{x_c}^2}, 0 \\ 0, \frac{1}{\sigma_{y_c}^2} \end{pmatrix} \tag{44}$$

Substituting (39) into (36) we obtain

$$f_{x_c, y_c} = K_{x_c} \exp\left(-\frac{1}{2} (\mathbf{e}_{x_c}^T J^T S_x^{-1} J \mathbf{e}_{x_c})\right) \tag{45}$$

where K_{x_c} represents a normalization of the output density and

$$J_{x_c} = J^T S_x^{-1} J = \begin{pmatrix} A & B \\ C & D \end{pmatrix}$$

where

$$A = \sum_{i=1}^6 \frac{1}{\sigma_{x_i}^2} J_{i1}^2; \quad B = \sum_{i=1}^6 \frac{1}{\sigma_{x_i}^2} J_{i1} J_{i2} \quad (46)$$

$$C = \sum_{i=1}^6 \frac{1}{\sigma_{x_i}^2} J_{i1} J_{i2}; \quad D = \sum_{i=1}^6 \frac{1}{\sigma_{x_i}^2} J_{i2}^2$$

Substitution of (46) into (45) leads with $B = C$ to

$$f_{x_c, y_c} = K_{x_c} \exp\left(-\frac{1}{2}(Ae_{x_c}^2 + De_{y_c}^2 + 2Ce_{x_c}e_{y_c})\right) \quad (47)$$

Comparison of (47) with (37) leads with (44) to

$$\rho = -\frac{C}{\sqrt{AD}}$$

$$\frac{1}{\sigma_{x_c}^2} = A - \frac{C^2}{D}; \quad \frac{1}{\sigma_{y_c}^2} = D - \frac{C^2}{A} \quad (48)$$

which is the counterpart to the 2 dim input case (24).

5.1 Fuzzy Approach

The first step is to compute values A_i , B_i and C_i from (46) at predefined positions/orientations $\mathbf{x} = (x_1, x_2, x_3, x_4, x_5, x_6)_i^T$. Then, we formulate fuzzy rules R_i , according to (33) and (34) with $i = 1 \dots n$, l - number of fuzzy terms, $k = 6$ - number of variables $n = l^k$ - number of rules. With such an increase in the number of inputs, one unfortunately sees the problem of an exponential increase in the number of rules, which is associated with a very high computational burden.

For $l = 7$ fuzzy terms for each input variable x_k , $k = 6$ we end up with $n = 7^6$ rules which is much to high to deal with in a reasonable way. So, one has to restrict to a reasonable number of variables at the input of a fuzzy system. This can be done either in a heuristic or systematic way (J.Schaefer and K.Strimmer, 2005) to find out the most influential input variables which is however not the issue of this paper.

6 MIXED GAUSSIAN DISTRIBUTIONS

For input signals with larger standard deviations one cannot assume that the fuzzy system is almost linear within the operating area. For this reason a distribution with large standard deviation is approximated by

several distributions with small standard deviations, where the linearization of the fuzzy system around their mean values applies. The following analysis applies with the analytical approach and the fuzzy approximation too. Let us concentrate on an example of a mixture of two distributions/densities f_{xy1} and f_{xy2}

$$f_{xy1} = \frac{1}{2\pi\sigma_{x_1}\sigma_{y_1}} \exp\left(-\frac{1}{2}\left(\frac{e_{x_1}^2}{\sigma_{x_1}^2} + \frac{e_{y_1}^2}{\sigma_{y_1}^2}\right)\right) \quad (49)$$

$$f_{xy2} = \frac{1}{2\pi\sigma_{x_2}\sigma_{y_2}} \exp\left(-\frac{1}{2}\left(\frac{e_{x_2}^2}{\sigma_{x_2}^2} + \frac{e_{y_2}^2}{\sigma_{y_2}^2}\right)\right) \quad (50)$$

that are linearly combined

$$f_{xy} = a_1 f_{xy1} + a_2 f_{xy2} \quad (51)$$

with $a_i \geq 0$ and $\sum_i a_i = 1$ where $i = 1, 2$ and

$$e_{x_1} = x_1 - \bar{x}_1; \quad e_{x_2} = x_2 - \bar{x}_2$$

$$e_{y_1} = y_1 - \bar{y}_1; \quad e_{y_2} = y_2 - \bar{y}_2$$

\bar{x}_i, \bar{y}_i are the mean values of x_i, y_i .

The partial outputs yield

$$f_{z_1, z_2}^i = \frac{1}{2\pi\sigma_{z_1}^i \sigma_{z_2}^i \sqrt{1 - \rho^{i2}}} \cdot \exp\left(-\frac{1}{2(1 - \rho^{i2})} \left(\frac{e_{z_1}^{i2}}{\sigma_{z_1}^{i2}} + \frac{e_{z_2}^{i2}}{\sigma_{z_2}^{i2}} - \frac{2\rho^i e_{z_1}^i e_{z_2}^i}{\sigma_{z_1}^i \sigma_{z_2}^i}\right)\right) \quad (52)$$

$e_{z_1}^i = z_1 - \bar{z}_1^i; e_{z_2}^i = z_2 - \bar{z}_2^i; \rho^i$ - correlation coefficient.

From this we finally obtain the output distribution

$$f_{z_1, z_2} = \sum_{i=1}^2 a_i f_{z_1, z_2}^i \quad (53)$$

The mixed output distribution f_{z_1, z_2} is a linear combination of partial output distributions f_{z_1, z_2}^i as a result of the input distributions $f_{x, y}^i$. Given the mean $\bar{z}_k^i, k = 1, 2$ and variance $\sigma_{z_k}^{i2}$ of the partial output distributions f_{z_1, z_2}^i . Then we find for mean and variance of the mixed output distribution

$$\bar{z}_k = \sum_{i=1}^2 \bar{z}_k^i \quad (54)$$

$$\sigma_{z_k}^2 = a_1(\sigma_{z_{k1}}^2) + a_2(\sigma_{z_{k2}}^2) + a_1 a_2 (\bar{z}_1 - \bar{z}_2)^2$$

from which we obtain the standard deviation σ_{z_k} of the intersection straight forward.

7 SIMULATION RESULTS

Gaussian Input Distributions.

Based on the human-robot intersection example, the following simulation results show the feasibility to predict uncertainties at possible intersections by using analytical and/or fuzzy models for a static situation (see fig. 2)). Position/orientation of robot and human are given by $\mathbf{x}_R = (x_R, y_R) = (2, 0)\text{m}$ and $\mathbf{x}_H = (x_H, y_H) = (4, 10)\text{m}$ and $\phi_R = 1.78$ rad, ($= 102^\circ$), and $\phi_H = 3.69$ rad, ($= 212^\circ$). ϕ_R and ϕ_H are corrupted with Gaussian noise with standard deviations (std) of $\sigma_{\phi_R} = \sigma_{x_1} = 0.02$ rad, ($= 1.1^\circ$). We compared the fuzzy approach with the analytical non-fuzzy approach using partitions of $60^\circ, 30^\circ, 15^\circ, 7.5^\circ$ of the unit circle for the orientations with results shown in table 1 and figures 5-8. Notations in table 1 are: $\sigma_{z_{1c}}$ - std-computed, $\sigma_{z_{1m}}$ - std-measured etc. The numbers show two general results:

1. Higher resolutions lead to better results.
2. The performance regarding measured and computed values depends on the shape of membership functions (mf's). Lower input std's (0.02 rad) require Gaussian mf's, higher input std's (0.05 rad = 2.9°) require Gaussian bell shape mf's which can be explained by different smoothing effects (see columns 4 and 5 in table 1).

Results 1 and 2 can be explained by the comparison of the corresponding control surfaces and the measurements (black and red dots) to be seen in figures 9 - 13. Figure 9 displays the control surfaces of x_c and y_c for the analytical case (4). The control surfaces of the fuzzy approximations (7) (see (Palm and Lilienthal, 2018)) are depicted in figures 10 - 13. Starting from the resolution 60° (fig. 10) we see a very high deviation compared to the analytic approach (fig. 9) which decreases more and more down to resolution 7.5° (fig. 13). This explains the high deviations in standard deviations and correlation coefficients in particular for sector sizes 60° and 30° .

Mixed Gaussian Distributions.

Due to larger uncertainties of the orientations of robot and human we assume the input signals to be a mixture of two Gaussian distributions with the following parameters:

$$\begin{aligned} \bar{\phi}_{R1} &= 1.779 \text{ rad}, (102 \text{ deg}), \sigma_{\phi_{R1}} = 0.02 \text{ rad} \\ \bar{\phi}_{H1} &= 3.698 \text{ rad}, (212 \text{ deg}), \sigma_{\phi_{H1}} = 0.02 \text{ rad} \\ \bar{\phi}_{R2} &= 1.762 \text{ rad}, (101 \text{ deg}), \sigma_{\phi_{R2}} = 0.03 \text{ rad} \\ \bar{\phi}_{H2} &= 3.716 \text{ rad}, (213 \text{ deg}), \sigma_{\phi_{H2}} = 0.03 \text{ rad} \end{aligned}$$

$$\begin{aligned} \sigma_{z_{11}} &= 0.1309 \text{ rad}; \sigma_{z_{21}} = 0.1157 \text{ rad} \\ \sigma_{z_{12}} &= 0.2274 \text{ rad}; \sigma_{z_{22}} = 0.1978 \text{ rad} \end{aligned}$$

Table 1: Standard deviations, fuzzy and non-fuzzy results.

input std sector size/ $^\circ$	0.02 Gauss, bell shaped (GB)				Gauss	0.05 GB
	60°	30°	15°	7.5°	7.5°	7.5°
non-fuzz $\sigma_{z_{1c}}$	0.143	0.140	0.138	0.125	0.144	0.366
fuzz $\sigma_{z_{1c}}$	0.220	0.184	0.140	0.126	0.144	0.367
non-fuzz $\sigma_{z_{1m}}$	0.160	0.144	0.138	0.126	0.142	0.368
fuzz $\sigma_{z_{1m}}$	0.555	0.224	0.061	0.225	0.164	0.381
non-fuzz $\sigma_{z_{2c}}$	0.128	0.132	0.123	0.114	0.124	0.303
fuzz $\sigma_{z_{2c}}$	0.092	0.087	0.120	0.112	0.122	0.299
non-fuzz $\sigma_{z_{2m}}$	0.134	0.120	0.123	0.113	0.129	0.310
fuzz $\sigma_{z_{2m}}$	0.599	0.171	0.034	0.154	0.139	0.325
non-fuzz $\rho_{z_{12c}}$	0.576	0.541	0.588	0.561	0.623	0.669
fuzz $\rho_{z_{12c}}$	-0.263	0.272	0.478	0.506	0.592	0.592
non-fuzz $\rho_{z_{12m}}$	0.572	0.459	0.586	0.549	0.660	0.667
fuzz $\rho_{z_{12m}}$	0.380	0.575	0.990	0.711	0.635	0.592

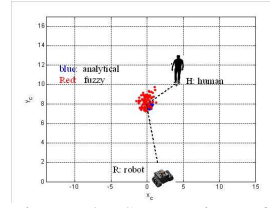


Figure 5: Sector size: 60 deg.

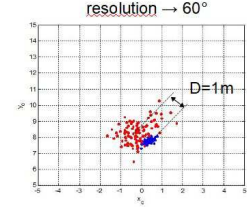


Figure 6: Sector size: 80 deg.

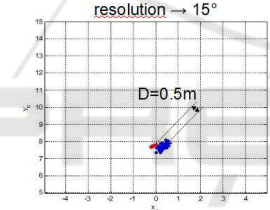


Figure 7: Sector size: 15 deg.

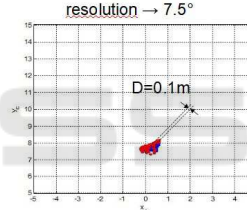


Figure 8: Sector size: 7.5 deg.

The following computed non-fuzzy and fuzzy (superscript F) and measured numbers (superscript m) according to (54) show the correctness of the previous analysis for the analytical case.

$$\begin{aligned} \bar{z}_1 &= 0.487; \quad \bar{z}_1^F = 0.413; \quad \bar{z}_1^m = 0.485 \\ \bar{z}_2 &= 7.746; \quad \bar{z}_2^F = 7.737; \quad \bar{z}_2^m = 7.737 \\ \sigma_{z_1} &= 0.222; \quad \sigma_{z_1}^F = 0.235; \quad \sigma_{z_1}^m = 0.199 \\ \sigma_{z_2} &= 0.184; \quad \sigma_{z_2}^F = 0.184; \quad \sigma_{z_2}^m = 0.178 \end{aligned}$$

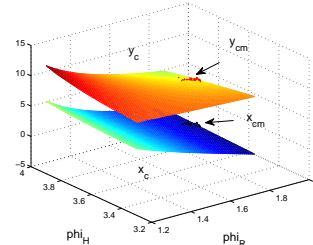


Figure 9: Control surface non-fuzzy.

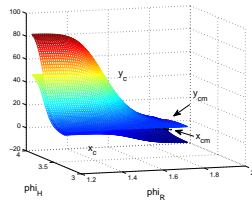


Figure 10: Control surface fuzzy, 60°.

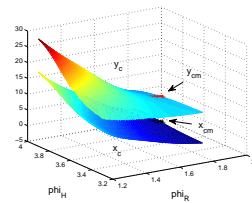


Figure 11: Control surface fuzzy, 30°.

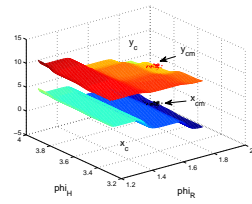


Figure 12: Control surface fuzzy, 15°.

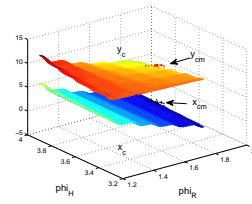


Figure 13: Control surface fuzzy, 7.5°.

Figures 14 and 15 show the regarding input and output densities where Figs. 16 and 17 depict the scatter diagrams (cuts at certain density levels). Finally it turns out that the fuzzy approximation is sufficiently accurate.

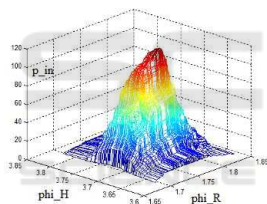


Figure 14: Mixed Gaussian, input.

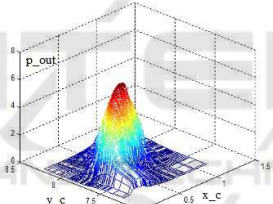


Figure 15: Mixed Gaussian, output.

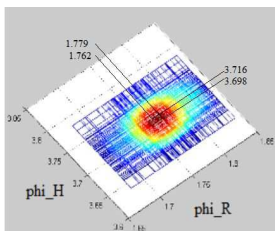


Figure 16: Scatter diagram, mixed input.

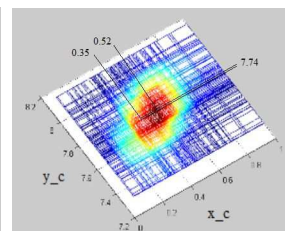


Figure 17: Scatter diagram, mixed output.

8 CONCLUSIONS

The work presented in this paper is motivated by the task to predict future situations such as collisions at specific areas in the presence of robots and humans and to use this information for feed forward control actions in the presence of uncertainties. This is essential for human intentions, actions and reactions that

are difficult to predict and interpret by a robot. We discussed the problem of intersections of trajectories in human-robot systems with respect to uncertainties that are modeled by Gaussian noise on the orientations of human and robot. This problem is solved by a transformation from human-robot orientations to intersection coordinates using a geometrical model and its TS fuzzy version. Based on the input standard deviations of the orientations of human and robot, the output standard deviations of the intersection coordinates are calculated. The analysis was performed under the condition that the nominal position/orientation of robot and human are constant and known. The measurements of their orientations are distorted by Gaussian noise with known parameters. This analysis together with the fuzzy extension also applies to robots and humans in motion, as long as the positions of robots and humans can be reliably estimated. We also extended our method to six inputs and two outputs which includes human/robot positions as well. For the analytical and the fuzzy version of two-input case the following inverse task can also be solved: given the standard deviation for the intersection coordinates, find the corresponding input standard deviations for the orientations of robot and human. For larger standard deviations of the orientation signals the method is finally extended to mixed Gaussian distributions. In summary, predicting the accuracy of human-robot cooperation at a small distance using the methods presented in this paper increases the system performance and human safety of human-robot collaboration. In future work this method will be used for robot-human scenarios in factory workshops and for robots working in difficult environments like rescue robots in cooperation with human operators.

ACKNOWLEDGMENT

This research work has been supported by the AIR-project, Action and Intention Recognition in Human Interaction with Autonomous Systems.

REFERENCES

- Banelli, P. (2013). Non-linear transformations of gaussians and gaussian-mixtures with implications on estimation and information theory. *IEEE Trans. on Information Theory*.
- Bruce, J., Wawer, J., and Vaughan, R. (2015). Human-robot rendezvous by co-operative trajectory signals. pages 1–2.
- Firl, J. (2014). Probabilistic maneuver recognition in traffic scenarios. *Doctoral dissertation, KIT Karlsruhe*.

- Fraichard, T., Paulin, R., and Reignier, P. (2014). Human-robot motion: Taking attention into account. *Research Report, RR-8487*.
- H.Hellendoorn and R.Palm (1994). Fuzzy system technologies at siemens r and d. *Fuzzy Sets and Systems 63 (3), 1994*, pages 245–259.
- J.Chen, Wang, C., and Chou, C. (2018). Multiple target tracking in occlusion area with interacting object models in urban environments. *Robotics and Autonomous Systems, Volume 103, May 2018*, pages 68–82.
- J.Schaefer and K.Strimmer (2005). A shrinkage to large scale covariance matrix estimation and implications for functional genomics. *Statistical Applications in Genetics and molecular Biology, vol. 4, iss. 1, Art. 32*.
- Kassner, M., W.Patera, and Bulling, A. (2014). Pupil: an open source platform for pervasive eye tracking and mobile gaze-based interaction. In *Proceedings of the 2014 ACM international joint conference on pervasive and ubiquitous computing*, pages 1151–1160. ACM.
- Khatib, O. (1985). Real-time obstacle avoidance for manipulators and mobile robots. *IEEE Int. Conf. On Robotics and Automation, St. Louis, Missouri, 1985*, page 500-505.
- L.Fouloy and S.Galichet (2003). Fuzzy control with fuzzy inputs. *IEEE Trans. Fuzzy Systems, 11 (4)*, pages 437–449.
- O.H.Hamid and N.L.Smith (2017). Automation, per se, is not job elimination: How artificial intelligence forwards cooperative human-machine coexistence. In *Proceedings IEEE 15th International Conference on Industrial Informatics (INDIN)*, pages 899–904, Emden, Germany. IEEE.
- Palm, R., Chadalavada, R., and Lilienthal, A. (2016). Fuzzy modeling and control for intention recognition in human-robot systems. In *7. IJCCI (FCTA) 2016: Porto, Portugal*.
- Palm, R. and Iliev, B. (2006). Learning of grasp behaviors for an artificial hand by time clustering and takagi-sugeno modeling. In *Proceedings FUZZ-IEEE 2006 - IEEE International Conference on Fuzzy Systems, Vancouver, BC, Canada. IEEE*.
- Palm, R. and Iliev, B. (2007). Segmentation and recognition of human grasps for programming-by-demonstration using time clustering and takagi-sugeno modeling. In *Proceedings FUZZ-IEEE 2007 - IEEE International Conference on Fuzzy Systems, London, UK. IEEE*.
- Palm, R. and Lilienthal, A. (2018). Fuzzy logic and control in human-robot systems: geometrical and kinematic considerations. In *WCCI 2018: 2018 IEEE International Conference on Fuzzy Systems (FUZZ-IEEE)*, pages 827–834. IEEE, IEEE.
- Pota, M., M.Esposito, and Pietro, G. D. (2011). Transformation of probability distribution into a fuzzy set interpretable with likelihood view. In *IEEE 11th International Conf. on Hybrid Intelligent Systems (HIS 2011)*, pages 91–96, Malacca Malaysia. IEEE.
- Robertsson, L., Iliev, B., Palm, R., and Wide, P. (2007). Perception modeling for human-like artificial sensor systems. *International Journal of Human-Computer Studies 65 (5)*, pages 446–459.
- R.Palm and Driankov, D. (1993). Tuning of scaling factors in fuzzy controllers using correlation functions. In *Proceedings FUZZ-IEEE'93, San Francisco, California. IEEE, IEEE*.
- R.Palm and Driankov, D. (1994). Fuzzy inputs. *Fuzzy Sets and Systems - Special issue on modern fuzzy control*, pages 315–335.
- Tahboub, K. A. (2006). Intelligent human-machine interaction based on dynamic bayesian networks probabilistic intention recognition. *Journal of Intelligent and Robotic Systems.*, Volume 45, Issue 1:31–52.
- W.Luo, J.Xing, Milan, A., Zhang, X., Liu, W., Zhao, X., and Kim, T. (2014). Multiple object tracking: A literature review. *Computer Vision and Pattern Recognition, arXiv 1409.7618*, page 1-18.
- Yager, R. and Filev, D. B. (1994). Reasoning with probabilistic inputs. In *Proceedings of the Joint Conference of NAFIPS, IFIS and NASA*, pages 352–356, San Antonio. NAFIPS.